

# Biosynthesis of silver and gold nanoparticles using *Trichoderma atroviride* for the biological control of *Phomopsis* canker disease in tea plants

ISSN 1751-8741  
 Received on 18th March 2016  
 Revised 21st May 2016  
 Accepted on 24th June 2016  
 E-First on 19th July 2016  
 doi: 10.1049/iet-nbt.2016.0029  
 www.ietdl.org

Ponnusamy Ponnuragan<sup>1</sup> ✉

<sup>1</sup>Department of Biotechnology, K.S.Rangasamy College of Technology, Tiruchengode 637 215, Namakkal District, Tamil Nadu, India

✉ E-mail: hodbt@ksrct.ac.in

**Abstract:** The biological way of metallic nanoparticles production using ecofriendly biocontrol agents are largely used to control many plant pathogenic microorganisms in agriculture. Hence, an attempt was made to evaluate the potential of suppressive activity of nanoparticles produced by an indigenous isolate, *Trichoderma atroviride* against a tea pathogenic fungus namely *Phomopsis theae*. The presence of biosynthesised nanoparticles was primarily confirmed through ultraviolet-visible spectroscopy analysis and was characterised using X-ray diffraction and scanning electron microscopy-energy dispersive X-ray analysis to delineate the size, shape and nature of particles. Further, Fourier transform infrared analysis revealed the functional biomolecules responsible for capping and stabilisation of nanoparticles. In addition, culture filtrate containing nanoparticles was subjected to *in vitro* antifungal studies which revealed a considerable suppression on the growth of *P. theae*. The biosynthesised nanoparticles were found to be active even after 3 months which established and confirmed the stability. Finally, field experiments conducted with soil application and wound dressing of nanoparticles exhibited a significant reduction in canker size when plants treated with gold followed by silver nanoparticles. Similarly, improvement in leaf yield was noted in response to these treatments. The above study confirmed the efficacy of metallic nanoparticles in management of stem disease in tea plantation.

## 1 Introduction

The use of microorganisms in the synthesis of nanoparticles emerges as an eco-friendly and exciting biological approach. There are investigation reports in which bacterium *Rhodospseudomonas capsulata* was employed and found successful to produce gold and silver nanoparticles (GN and SN) of different sizes and shapes [1]. Therefore, synthesis of these nanoparticles of different sizes and shapes is of great importance for their application in plant disease control. An earlier study found that stabilisation of SN and GN due to the surface-active molecules released by *Bacillus subtilis* [2]. In general, fungi such as *Verticillium lecanii* and *Fusarium oxysporum* and actinomycetes such as *Streptomyces*, and other microbes *Thermomonospora* and *Rhodococcus* spp. were also used to synthesise SN and GN intra and extracellularly. However, the biosynthesis of GN and SN is still scarce. In this study, eukaryotic fungi *Trichoderma atroviride* recognised as one of the ecologically and environmentally important biocontrol agent commonly used to control many plant diseases was selected as reducing agent for metallic nanoparticle synthesis.

Tea, the most popular beverage in the world, obtained from the flush shoots of the plant *Camellia sinensis* (L). O. Kuntze. It is considered to be the chief commercial crop in India and it occupies a vital place in national economy. Humid climatic conditions and heavy rainfall lead to exposure of many fungal diseases, among which *Phomopsis* canker caused by *Phomopsis theae* Petch is the major constraint and leads to considerable economic losses in tea plantations. The pathogen seems to be prevalent in mature tea fields rather than young tea plantations [3]. Infected bushes are being cleared and replanted with clonal tea later in the replanting and refilling planting programmes [4]. In order to control the disease, fungicides are frequently recommended, but may have adverse influence on the environment and non-targeted organisms [5]. Avoidance of pre-disposing factors and uproot and burning of the bushes in severe cases are also recommended as a control measure [6]. Despite its significance, effective control measures are not available other than pruning to healthy wood and application of copper fungicides on prune cuts [7]. The applications of systematic

fungicides are mostly toxic, non-degradable and pollute the atmosphere by spread out in the air and amass in the soil. The repeated use of such chemicals may encourage the development of chemical resistance in target organisms [8].

Biological control of plant pests and pathogens continues to instigate research and development in numerous fields especially in plantation crops like tea plants. A large number of plant diseases were successfully controlled through bacterial and fungal antagonists. Soil application and wound dressing of biocontrol agents such as *Trichoderma harzianum* and *Gliocladium virens* were found to be superior to fungicides in controlling *Phomopsis* canker under field condition. Moreover imposing of treatments containing these two biocontrol agents enhanced bud break, tipping weight and green leaf yield potential in the trail plots [4]. However, only meager information is available on the biological control of tea diseases using nanoparticles which are synthesised from biocontrol agents. The nanoparticles synthesised from antagonists have received special attention in terms of controlling plant diseases due to long shelf life and stability. Additionally, the SN and GN possess an excellent biocompatibility and low toxicity and they have antibacterial/antifungal properties. Silver (Ag) has been known to exhibit strong toxicity to wide range of microorganisms in terms of antibacterial and antifungal applications [9]. To keep in mind, an attempt was made to produce SN and GN in the culture filtrate of *T. atroviride* under *in vitro* condition. This experimentation will be of more useful later to evaluate the efficacy of these two nanoparticles against *Phomopsis* canker under field condition after preparing suitable carrier-based bioformulation.

## 2 Materials and methods

### 2.1 Culture of biocontrol agent and preparation of inoculum

*T. atroviride* (MTCC No.9641) was grown in Erlenmeyer flask containing *Trichoderma* selective medium for 25 days under shaking condition (200 rpm) at 27°C. After incubation, the mycelial biomass was then separated from the broth by

centrifugation (500 rpm) and washed thrice with sterilised double distilled water.

## 2.2 Biosynthesis of SN and GN

The harvested mycelial biomass about 500 mg was exposed to 50 ml aqueous solution of  $2 \times 10^{-3}$  M chloroauric acid for GN production and 75 ml aqueous solution of  $3 \times 10^{-4}$  M silver nitrate for SN production in Erlenmeyer flask containing 250 ml medium at pH 5.5. The whole mixture was put into an orbital shaker (200–250 rpm) and reaction was carried out for 3–10 days.

## 2.3 Characterisation of nanoparticles by UV-visible (UV-vis) spectroscopy

The bioreduction of metal ions was monitored by visual inspection of the solution and biomass as well as by measuring the intensity of the solution from 300 to 700 nm using Hitachi spectrophotometer. In order to identify SN production, the colour of the reaction solution turned from pale yellow to purple colour from the fifth day of incubation onwards and turned dark brown by the end of the tenth day. Similarly, in the case of GNs, the colour of the reaction solution turned from pale green to dark yellow colour from the fifth day of incubation onwards [10].

## 2.4 Scanning electron microscopy (SEM)-energy dispersive X-ray (EDX) spectrometry analysis of nanoparticles

The nanoparticles biosynthesised by *T. atroviride* were subjected to SEM-EDX characterisations following the method of Sastry *et al.* [11]. Analysis of SN and GN using SEM was carried out using JEOL-MODEL 6390 special edition machine compatible with EDX machine. The pellet was dried in an oven and thin films of dried samples (10 mg/ml) were prepared on carbon coated copper grid and analysed for size determination. While, the extra solution was removed using a blotting paper and then the films on the SEM grid were allowed to dry by putting it under a mercury lamp for 5 min. The particle size and texture of nanoparticles can be analysed by using image magnification software compatible with SEM and helps in determining the presence and formation of SNs.

## 2.5 Characterisation of nanoparticles using X-ray diffraction (XRD) and Fourier transform infrared (FTIR) spectroscopy

The aliquots of silver nitrate and chloroauric acid treated nano-*T. atroviride* biomass containing culture filtrates were taken and their absorption was measured in a microplate reader (Electronics Corporation of India, Hyderabad, India). The solution was then converted into powder for XRD measurements. XRD pattern was obtained from lyophilised culture filtrate containing GN and SNs by powder diffraction method, where it gives grain size and shape of the particles by h, k and l index value. The samples were coated on the XRD grid and the spectra were recorded by X-ray diffractometer (Electronics Corporation of India, Hyderabad, India). The FTIR spectroscopy was performed to the culture filtrate which was exposed before and after addition to the  $\text{AgNO}_3$  and  $\text{AuCl}_4$  solution. The samples were mixed with KBr to make a pellet and it was placed in the sample holder. The spectrum was recorded at a resolution of  $4 \text{ cm}^{-1}$  [12, 13].

## 2.6 In vitro antifungal activity and shelf-life study of biosynthesised nanoparticles

The culture filtrate containing SN and GN biosynthesised by *T. atroviride* was taken up for the present study. Petridishes containing potato dextrose agar (PDA) medium supplemented with 10% above biosolution was centrally inoculated with 5 mm disc size of 7 day old test pathogen, *P. theae*. After every 24 h of incubation at room temperature, the radial growth of the pathogen was measured using a metric scale for a period of 7 days and calculated for inhibition percentage [14]. Pathogen inoculated on PDA plates containing distilled water devoid of supplementing nanoparticles served as control. The culture filtrate containing

nanoparticles was maintained up to 3 months to check out the stability of nanoparticles towards antagonistic potential.

## 2.7 Field location and treatments

Field experiments were conducted in naturally infected *Phomopsis* canker disease tea fields at two different estates of Parry Agro Tea Industries, Valparai, Tamil Nadu, India during 2012–2015 in the Western Ghats of southern India ( $10^{\circ}30'N$ ,  $77^{\circ}0'E$ , altitude 1050 m above MSL). Susceptible clone UPASI-9 with a population of 15,000 plants/ha was studied. The field experiments were devised as completely randomised block designs. Each experiment consisted of 10 treatments and each plot consisted of 30 bushes. Systemic fungicides such as hexaconazole applied at the rate of 0.05% with 1l/bush and for wound dressing, copper oxychloride and mancozeb were made into a paste with linseed oil (1:1 ratio) and applied to the cankered region with a brush. SN and GN were sprayed on *P. theae* infected plants applied at the different rate of 1–3 ppm concentration with 1.5 l/bush. For wound dressing, a talc preparation was made where the above nanoparticles were mixed with commercial talc along with carboxymethyl cellulose (0.5%) as an adhesive agent. The talc preparation was made into a paste with distilled water (1:2 ratio) and applied to the pruned cuts and cankered portion with a brush. The same application was followed for bulk nanoparticles [15].

## 2.8 Disease assessment

The disease incidence was recorded on 30 bushes (30 canker region) selected randomly per treatment. Disease assessment was recorded two times per year during pre monsoon (April and May) and post monsoon (November and December) seasons. Length and breadth of canker size was measured using metric scale. Disease incidence was calculated by measuring the size of canker (length and width) and  $\text{PDI} = \text{canker size of pre treatment} - \text{canker size of post treatment} / \text{canker size of pre treatment} \times 100$  [4].

## 2.9 Green leaf yield assessment

Yield data per plot were recorded regularly during the course of the experimental period. Yield and yield attributes in terms of productivity index were monitored at every plucking round. The green leaf yield was converted to made tea in kilogram per hectare ( $\text{kg ha}^{-1}$ ) by the formula,  $\text{yield} = \text{green leaf yield (kg)} \times 15,000 \times 0.225 / \text{number of bushes in the experimental plot}$ , where 15,000 is the total bush number per hectare and 0.225 is the conversion factor for green leaf (22.5% out turn) to made tea [16].

## 3 Results

The UV absorption spectral study was carried out initially to confirm the formation of SN and GN synthesised by *T. viride*. The result indicated that existence of SNs was profound in the culture filtrate when measured at 410 nm. In the case of GNs, it was observed highly at 450 nm and thereafter there was a sharp decline in the absorbance (Fig. 1). It has been noted that the stability of biosynthesised SN and GN was constant ever after 3 months of incubation in culture filtrate. After 1 month of incubation under dark room condition, yellow coloured reaction mixture turned into dark brown colour. In the case of GNs, the sample solution turned from light yellow to golden brownish colour.

Analysis of SEM showed the presence of Ag and gold particles in nano size ranging  $<100$ – $200$  nm as depicted in Fig. 2. The nanoparticles showed that nearly 60% of the total nanoparticle population is due to triangular gold nanoplates in the size of 50–75 nm. It has been noticed that most of the other nanoparticles are spherical in shape with a size ranged between 10 and 50 nm.

Analysis through EDX spectrum confirmed the presence of elemental Ag and Au by exhibiting the peaks at their characteristic energy levels. The vertical axis displays the number of X-ray counts whilst the horizontal axis displays energy in kiloelectronvolts (keV). Identification lines displayed for the major emission energies for Ag correspond to the peaks obtained in the spectrum; thus, giving confidence that Ag has been correctly identified

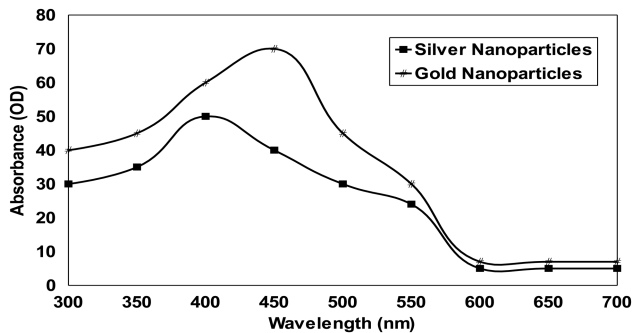


**Fig. 1** Absorption spectra of biosynthesised SN and GN by *T. atroviride*

clearly in which peaks located between 2 and 4 keV. Those maxima are directly related to the Ag characteristic (Fig. 2a). Similarly, an absorption peak obtained at ~2 keV which is specifically related to characteristic of GNs obtained in the spectrum (Fig. 2b). The mass of Ag ranged from 7.24 to 13.27% with atom of about 2.95–11.17% whereas for gold, it ranged from 14.09 to 25.23% with

atom of 5.6–10.78%. The GN and SN were found to be crystalline with oval and spherical shape, respectively.

The XRD pattern revealed that the SNs synthesised by the antagonists have broad peaks due to nano crystalline in nature. In contrast, all the GNs revealed micro/macro crystalline nature by the presence of clear distinct peaks. The crystallite size calculated by subjecting the  $2\theta$  (peak position) and full width at half maximum (width of half peak height) values of major peaks in Debye–Scherrer equation varied from 10.26 to 35.03 nm (Fig. 3) In our study, SNs was exhibited with the broad peaks at  $27.44^\circ$ ,  $31.93^\circ$  and  $46.98^\circ$  which corresponded to 110, 111 and 210 planes, respectively. Similarly, GNs were noticed with peaks  $2\theta$  (degree) as  $17.17^\circ$ ,  $23.68^\circ$ ,  $38.02^\circ$  and  $46.12^\circ$  which correspond to the (111), (200) and (311) planes of the standard cubic phase of gold. The FTIR analysis revealed characteristic functional biomolecules present in SN and GN samples (Fig. 4). The bands between  $3600\text{--}3300\text{ cm}^{-1}$  and  $3000\text{--}2800\text{ cm}^{-1}$  were assigned to stretching vibrations of primary and secondary amines. The corresponding bending vibrations were also observed in the range of  $1700\text{--}1640\text{ cm}^{-1}$  and  $1600\text{--}1400\text{ cm}^{-1}$ . These spectral peaks obtained were found to be similar pattern throughout the experimentation period

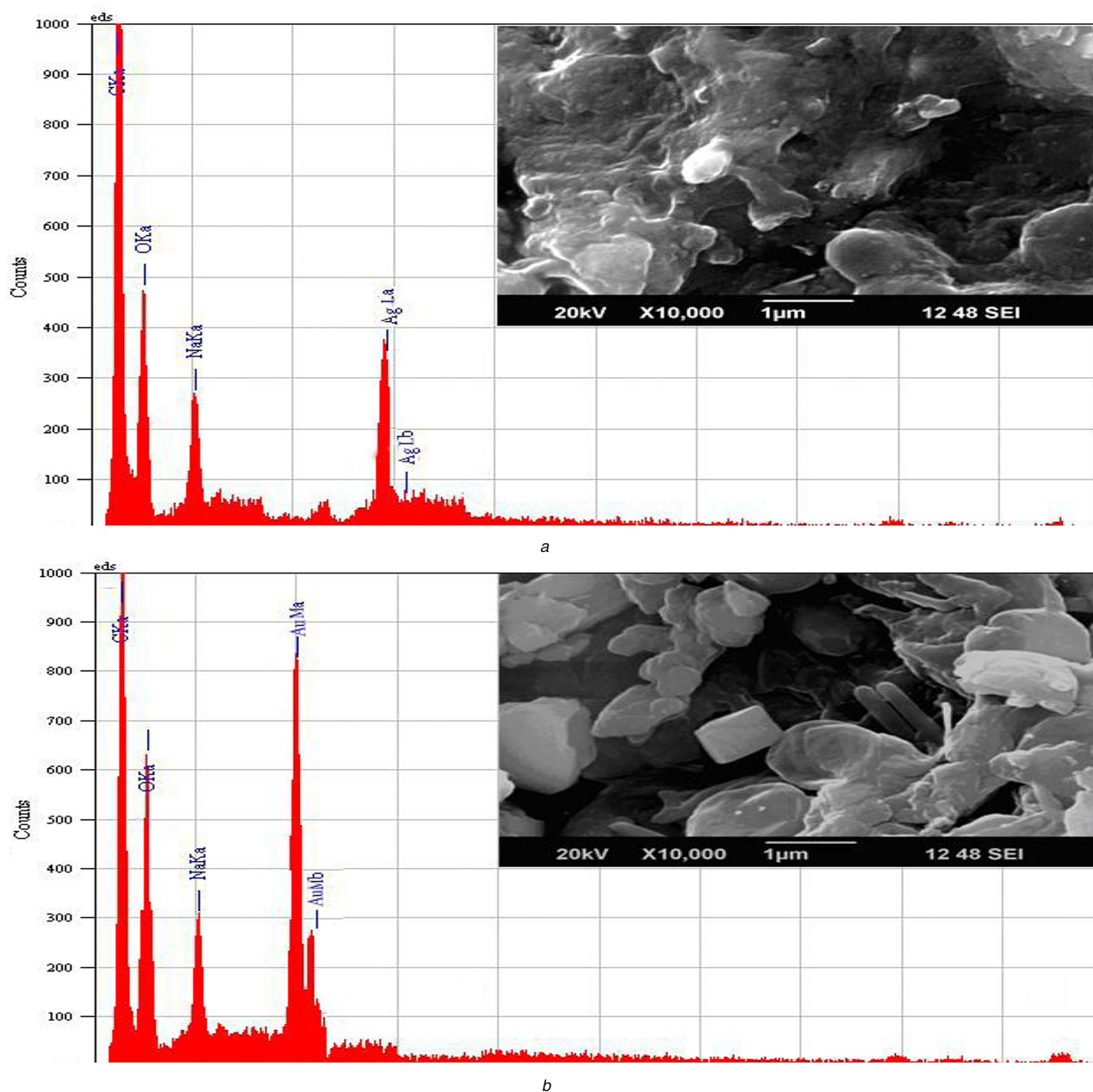


**Fig. 2** Characterisation of different nanoparticles by SEM-EDX (a) SNs, (b) GNs

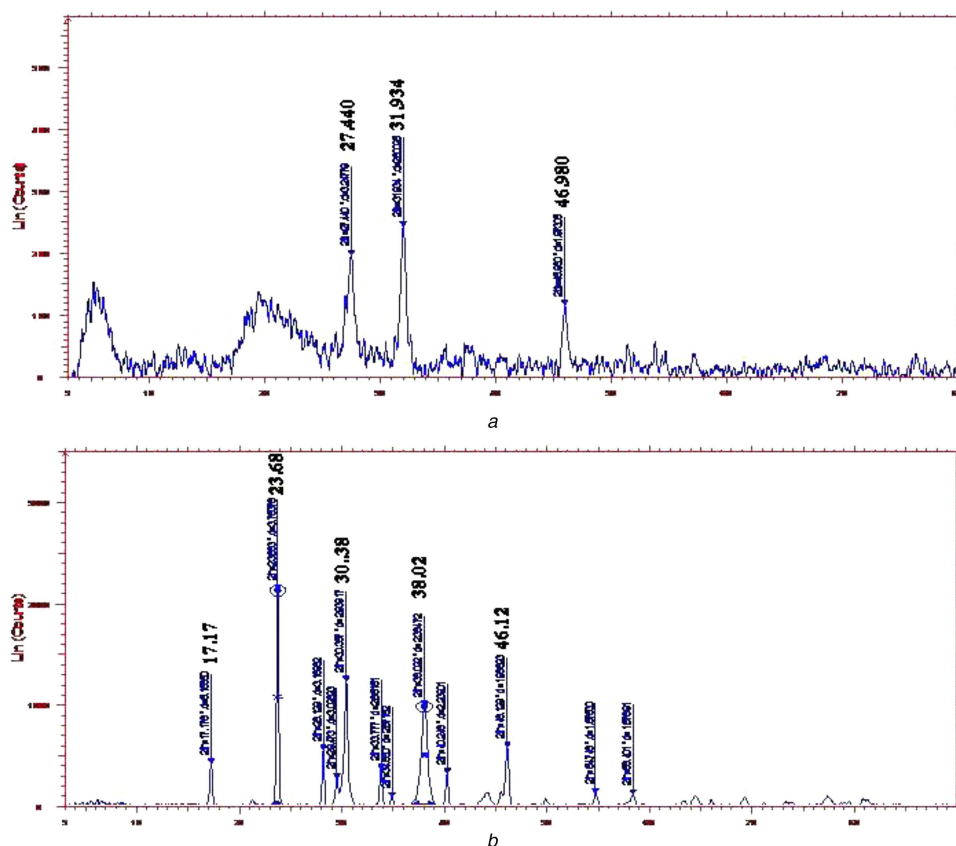


**Fig. 3** XRD spectrum analysis of different nanoparticles  
(a) SNs, (b) GNs

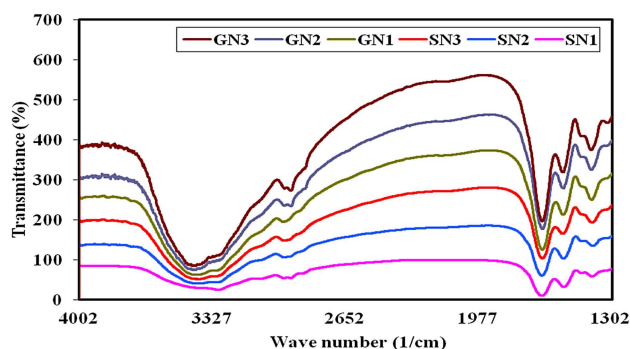


**Fig. 4** FTIR characterisation of nanoparticles synthesised by *T. atroviride* during different month intervals (at every 6 month intervals)  
GN – Gold nanoparticle; SN – Ag nanoparticle

of three months which may be related to the stability of the nanoparticles.

### 3.1 Antifungal activity of biosynthesised nanoparticles and its shelf-life

The mycelial growth inhibition of *P. theae* by biosynthesised nanoparticles under solid medium gradually increased from first day onwards and finally reached up to seventh day of incubation and thereafter it was stable up to 3 months (Table 1). The growth inhibition of the pathogen was superior to untreated control plates due to absence of nanoparticles. The maximum growth inhibition was 75.7% in SN and 80.3% in GN which was used for the biological control of *P. theae* on seventh day of incubation. Among the two nanoparticles tested for growth inhibition of the pathogen, GNs was found to be higher when compared with SNs biosynthesised by *T. atroviride*. The shelf-life of both nanoparticles synthesised from *T. atroviride* was studied over a period of 3 months which revealed inhibition of *P. theae* by SNs was registered between 74.7 and 75.7% while it was in the range of 80.3 and

79.6% in GNs treatment. On the other hand, there was no growth inhibition of *P. theae* in control treatment after 3 months of incubation (Table 2). The growth inhibition was found to be superior in culture filtrate containing GNs than in Ag.

### 3.2 Effect of nanoparticles application on disease incidence and leaf yield of tea plants

In response to soil drenching and wound dressing of fungicide, bulk metals and nanoparticles (at different dosage), there was a significant reduction in *Phomopsis* canker (Table 3). Plants treated with hexaconazole showed superior disease control which accounted for 69.27% of disease reduction. On the contrary, bulk nanoparticles (Ag and gold) treated plants exhibited inferior control when compared with fungicides. Among the varying concentration of nanoparticles applied, the maximum disease control was observed at 2 ppm dosage with 60.91% disease reduction in case of GNs whereas SNs was noted with 56.83% disease reduction when compared with untreated control – 119.80%. In contrast, among ten different treatments, the highest leaf yield of 3565 kg ha<sup>-1</sup> made tea was recorded in the treatment containing nanogold at 2.0 ppm concentration. This was followed by treatment with nano Ag at 3.0 ppm with 3256 kg ha<sup>-1</sup> made tea. The infected control was noticed with defoliation and heavy flowering where the highest disease incidence, lowest disease protection and least leaf yield were recorded (Table 3).

## 4 Discussion

GN and SN synthesised by various techniques have received special attention because they have found potential application in many fields such as catalysis, sensors, drugs delivery system and stability. Additionally, these nanoparticles possess an excellent biocompatibility and low toxicity with various bioformulations and they have prominent antibacterial/antifungal properties.

In our current study, UV-vis spectroscopy studies showed peak absorption at 410 and 450 nm revealed the presence for SN and GN. It may be due to the excitation of surface plasmon resonance

**Table 1** Antagonistic potential of *T. atroviride* culture filtrate containing SN and GN on the growth inhibition of *P. theae*

Days after inoculation	Radial growth of <i>P. theae</i> , mm			standard error $\pm$	critical difference at $P = 0.05$
	SN	GN	Untreated control		
1	6 <sup>b</sup>	5 <sup>b</sup>	18 <sup>a</sup>	0.81	0.01
2	8 <sup>b</sup>	7 <sup>b</sup>	30 <sup>a</sup>	0.93	0.00
3	11 <sup>b</sup>	8 <sup>c</sup>	42 <sup>a</sup>	1.53	0.02
4	14 <sup>b</sup>	10 <sup>c</sup>	54 <sup>a</sup>	1.87	0.01
5	17 <sup>b</sup>	13 <sup>c</sup>	66 <sup>a</sup>	2.19	0.04
6	20 <sup>b</sup>	15 <sup>c</sup>	78 <sup>a</sup>	2.36	0.03
7	22.0 <sup>b</sup>	18.0 <sup>c</sup>	90 <sup>a</sup>	2.72	0.02
percentage of inhibition, % <sup>a</sup>	75.7 <sup>b</sup>	80.3 <sup>a</sup>	—	2.90	0.00

<sup>a</sup>Percentage of inhibition (%) was calculated on seventh day after inoculation.

Mean values in each column followed by different letters are significantly different at  $P < 0.05$ , according to DMRT.

**Table 2** Shelf life of *T. atroviride* culture filtrate containing SN and GN on the growth inhibition of *P. theae*

<i>Trichoderma</i> culture filtrate containing <sup>a</sup>	Growth inhibition of <i>P. theae</i> , %									
	Days									
	10	20	30	40	50	60	70	80	90	
SNs	75.7 <sup>b</sup>	75.7 <sup>b</sup>	75.5 <sup>b</sup>	75.3 <sup>b</sup>	75.3 <sup>b</sup>	75.1 <sup>b</sup>	75.1 <sup>b</sup>	74.9 <sup>b</sup>	74.7 <sup>b</sup>	
GNs	80.3 <sup>a</sup>	80.3 <sup>a</sup>	80.3 <sup>a</sup>	80.1 <sup>a</sup>	80.1 <sup>a</sup>	79.8 <sup>a</sup>	79.7 <sup>a</sup>	79.6 <sup>a</sup>	79.6 <sup>a</sup>	
SE $\pm$	2.31	2.47	2.15	2.63	1.74	1.48	2.08	1.52	1.86	
CD at $P = 0.05$	0.03	0.01	0.00	0.02	0.04	0.02	0.01	0.00	0.03	

<sup>a</sup>Percentage of inhibition (%) was calculated on seventh day after inoculation.

Mean values in each column followed by different letters are significantly different at  $P < 0.05$ , according to Duncans multiple range test.

**Table 3** Impact of biosynthesised SN and GN on *Phomopsis* canker and leaf yield in tea plants

T. number	Treatments	Canker size, cm				Disease reduction, %	Yield, kg ha <sup>-1</sup> made tea
		Pre treatment		Post treatment			
		Length	Width	Length	Width		
T1	hexaconazole – 0.05%	6.8 <sup>a</sup>	2.8 <sup>a</sup>	4.5 <sup>e</sup>	1.3 <sup>e</sup>	69.27 <sup>a</sup>	3564 <sup>b</sup>
T2	bulk Ag	6.1 <sup>a</sup>	2.6 <sup>a</sup>	5.9 <sup>b</sup>	2.2 <sup>b</sup>	18.15 <sup>g</sup>	2714 <sup>ef</sup>
T3	bulk gold	6.3	2.7 <sup>a</sup>	6.0 <sup>b</sup>	2.4 <sup>b</sup>	15.34 <sup>i</sup>	2822 <sup>de</sup>
T4	nanosilver – 1 ppm	6.0 <sup>a</sup>	2.3 <sup>a</sup>	5.8 <sup>b</sup>	2.0 <sup>bc</sup>	15.94 <sup>h</sup>	3039 <sup>c</sup>
T5	nano Ag – 2 ppm	6.4 <sup>a</sup>	2.5 <sup>a</sup>	5.6 <sup>bc</sup>	2.1 <sup>bc</sup>	26.5 <sup>e</sup>	2873 <sup>cde</sup>
T6	nanosilver – 3 ppm	6.7 <sup>a</sup>	2.6 <sup>a</sup>	4.7 <sup>de</sup>	1.6 <sup>cde</sup>	56.83 <sup>c</sup>	3682 <sup>ab</sup>
T7	nanogold – 1 ppm	6.2 <sup>a</sup>	2.4 <sup>a</sup>	5.9 <sup>b</sup>	1.9 <sup>bcd</sup>	24.66 <sup>f</sup>	2957 <sup>cd</sup>
T8	nanogold – 2 ppm	6.5 <sup>a</sup>	2.7 <sup>a</sup>	4.9 <sup>de</sup>	1.4 <sup>de</sup>	60.91 <sup>b</sup>	3765 <sup>a</sup>
T9	nanogold – 3 ppm	6.6 <sup>a</sup>	2.8 <sup>a</sup>	5.2 <sup>cd</sup>	2.3 <sup>b</sup>	35.28 <sup>d</sup>	3548 <sup>b</sup>
T10	infected control	6.9 <sup>a</sup>	2.7 <sup>a</sup>	9.1 <sup>a</sup>	4.5 <sup>a</sup>	-119.80 <sup>j</sup>	2561 <sup>f</sup>
SE $\pm$		0.11	0.09	0.23	0.16	5.83	79.40
CD at $P = 0.05$		0.01	0.00	0.02	0.01	0.02	0.03

Mean values in each column followed by different letters are significantly different at  $P < 0.05$ , according to DMRT test.

for the synthesised SNs. The nanoparticles exhibit unique and tunable optical properties on account of their surface plasmon resonance, dependent on shape and size distribution of the nanoparticles. Previous studies reported that a bacterium *R. capsulata* is known to secrete cofactor NADH- and NADH-dependent enzymes that may be responsible for the bioreduction of Au(3+) to Au (0) and the subsequent formation of GNs [10, 17]. Similar studies were carried out by Gopinath *et al.* [12] who demonstrated that use of *Tribulus terrestris* extract as a reducing agent can effectively produce the crystalline with oval and spherical shape gold and SNs followed by the green chemistry approach. The synthesised nanoparticles proved excellent antimicrobial activity against pathogen microorganisms and found to be stable after 6 months in room temperature.

SEM analysis generally provide an in depth image resolution of the particles by rastering a focussed electron beam across the surface and detecting secondary or backscattered electron signal. In contrast, EDX is also used to provide elemental identification and

quantitative compositional information. In our study, surface analysis, topology, structural arrangement and energy dispersion of biosynthesised nanoparticles were studied through SEM-EDX. Previously, Dinesh *et al.* [18] reported that SEM and the EDX analysis showed polydispersed SNs captured with the high resolution images which indicated good crystallinity of the nanoparticles and similarly, strong signal in the Ag region which confirmed the SNs formation. It has been confirmed from these studies that metallic Ag nanocrystals generally show typical optical absorption peak approximately at 3 keV due to surface plasmon resonance.

Earlier, Chitra and Annadurai [19] confirmed the crystalline nature of the nanoparticles through XRD studies. In parallel, our biosynthesised nanoparticles of diffraction pattern exhibited relative size and shape produced from the peak intensities. On overall, the compound involved in reduction of Ag and gold ions contains unsaturated – simple hydroxyl-amide group suggesting to be a hydrolysing protein or enzyme that is reported in many

antagonist. Hence, it may be assumed that these biomolecules are responsible for capping and efficient stabilisation. Similarly, according to findings of Badri Narayanan and Sakthivel [20] the presence of reducing sugars in the extract could be responsible for the reduction of metal ions and formation of the nanoparticles.

In general, XRD method is commonly used for determining the chemical composition and crystal structure of a material. It also provides information on translational symmetry – size and shape of the unit cell from peak positions, deviation and electron density inside the unit cell, namely where the atoms are located from peak intensities. In our experiment, the X-ray pattern of biosynthesised SN and GN was achieved by observing the pattern of diffraction peaks exhibited from the metallic particles. The diffraction peaks obtained in XRD corresponded to face centred cubic structure of metallic Ag ions in its purest form. This finding was coincided with previous work of Khatami *et al.* [21] who confirmed the formation of the nanocrystalline Ag by the XRD analysis biosynthesised from seed exudates of *Sinapis arvensis*. Likewise, according to Soltani Nejad *et al.* [22], the biosynthesised GNs using *Streptomyces fulvissimus* was characterised and confirmed through diffraction peaks for the GNs indicated that GNs were in clear and pure form crystalline in this size range while its broadening is related to the particles in the nanometer size regime.

FTIR measurements were carried out in order to obtain information about chemical groups present around nanoparticles for their stabilisation and understand the transformation of functional groups due to reduction process. According to Banala *et al.* [23], FTIR analysis of SN showed sharp absorption peaks indicating the possible interaction between proteins and SNs and could be due to the amide bond coming from the carbonyl group of a protein and OH groups present in alcohols and phenolics. Similarly, Batal *et al.* [24] findings suggested the FTIR spectral analysis of GNs, indicated that the nanoparticles synthesised using the soybean-garlic fermented extract are surrounded by proteins, sulphone groups and metabolites such as polyphenols having functional groups of alcohols, amines and carbonyl which facilitate the reduction of gold ions to respective nanoparticles. The above studies were in parallel to our reports and also revealed that biosynthesised nanoparticles were surrounded by various chemical and functional groups which are responsible for stabilisation and capping of particles.

In general, both SN and GN biosynthesised from antagonistic fungi have been known to exhibit strong toxicity to wide range of pathogenic microorganisms in terms of antibacterial and antifungal properties (Chang *et al.* [25]; Rai *et al.* [9]). In our study, antifungal activity against *P. theae* was more pronounced in culture filtrate containing GNs than in SNs (Table 1). GN-bound DNA towards various biological, physical and chemical agents were studied and reported to be the most stable one with long shelf-life to deliver the antifungal compounds by encapsulation [17]. Antimicrobial activity of GNs biosynthesised from fungal and bacterial biocontrol agents studied against *E. coli* (ATCC 25922 strain) by Azam *et al.* [26] revealed that the growth of *E. coli* was inhibited excellently under *in vitro* even after 18 months. Stability conferred by GNs gave long-term antagonistic activity against *P. theae*, which possibly provide a suitable option for the control of *Phomopsis* canker disease in tea plantations.

This growth inhibition might be due to the diffusible metabolites with low molecular weight secreted by the antagonist according to the reports of Fernando *et al.* [27]. Moreover, diffusible metabolites were highly stable up to 2 months due to SN and GN reaction [11, 28]. The antagonistic activity of *T. atroviride* on pathogen growth was significantly inhibited due to colonisation of the antagonist and involvement of cell wall lytic enzymes secreted by antagonist which was earlier studied by Dadrick *et al.* [29]. The inhibition by the bioassay of SN and GN was due to adherence of these nanoparticles upon the surface of cell membrane and drastically disturbs its proper function like respiration and permeability and causes lysis of cells subsequently [30].

Earlier Kim *et al.* [31] reported the spray method delivery of colloidal SNs against powdery mildew caused by *Sphaerotheca pannosa* var. *rosae* in white rose plants under greenhouses

condition. A significant antifungal activity with effective disease control was observed in response to nanoparticles application. On contrary, in our study soil drenching and wound dressing of SN and GN in *P. theae* infected stem resulted in considerable reduction of canker size. In addition, appreciable increase in leaf yield was observed with respect to application of Ag and gold treated plants when compared with untreated plants.

## 5 Conclusion

In the present study, GN and SN were synthesised from a potential antagonistic fungus *T. atroviride*. These two nanoparticles were tested for antagonistic activity against a tea fungal pathogen *P. theae*. The growth inhibition of the pathogen was significantly registered with nanoparticles rather than untreated control. Further, the synthesised nanoparticles were characterised by FTIR, XRD spectrum and SEM-EDX analysis to study the nature size and shape. Finally, the field application of these two nanoparticles had significant impact over disease control as well as improvement in leaf yield. Therefore, it has been concluded that biologically synthesised nanoparticles may be a more rapid and environmental friendly approach for disease control than current approaches.

## 6 Acknowledgment

The author gratefully acknowledges the National Tea Research Foundation (NTRF), Kolkata for financial support to carry out this study.

## 7 References

- He, S., Zhirui Guo, Z., Zhang, Y., *et al.*: 'Biosynthesis of gold nanoparticles using the bacteria *Rhodospseudomonas capsulate*', *Mater. Lett.*, 2007, **61**, pp. 3984–3987
- Reddy, A.S., Chen, C.Y., Chen, C.C., *et al.*: 'Biological synthesis of gold and silver nanoparticles mediated by the bacteria *Bacillus subtilis*', *J. Nanosci. Nanotechnol.*, 2010, **10**, (10), pp. 6567–6574
- Bore, K.A.J.: 'A review of problems of old tea fields', *Tea*, 1996, **17**, pp. 27–33
- Ponmurugan, P., Baby, U.I.: 'Evaluation of fungicides and biocontrol agents against *Phomopsis* canker of tea under field condition', *Aust. J. Plant Pathol.*, 2007, **36**, pp. 68–72
- Brimner, T.A., Boland, G.J.: 'A review of the non-target effects of fungi used to biologically control plant diseases', *Agri. Ecosyst. Environ.*, 2003, **100**, pp. 3–16
- Baby, U.I., Ponmurugan, P., Premkumar, R., *et al.*: 'Incidence of *Phomopsis* canker in south Indian tea plantations', *Planter's Chronicle*, 2001, **97**, pp. 303–307
- Ponmurugan, P., Baby, U.I.: 'Management of *Phomopsis* canker of tea with fungicides and biocontrol agents', *J. Plantm Crops*, 2006, **33**, pp. 175–178
- Naseby, D.C., Pascual, J.A., Lynch, J.M.: 'Effect of biocontrol strains of *Trichoderma* on plant growth, *Pythium ultimum* population, soil microbial communities and soil enzyme activities', *J. Appl. Microbiol.*, 2006, **88**, pp. 161–169
- Rai, M., Yadav, A., Gade, A.: 'Silver nanoparticles as a new generation of antimicrobial', *Biotech. Adv.*, 2009, **27**, pp. 76–83
- Mukherjee, P., Roy, M., Mandal, B.P., *et al.*: 'Green synthesis of highly stabilized nanocrystalline silver particles by a non-pathogenic and agriculturally important fungus *T. spereillum*', *Nanotechnology*, 2008, **19**, pp. 1–7
- Sastry, M., Ahmad, A., Khan, M.I., *et al.*: 'Biosynthesis of metal nanoparticles using fungi and actinomycetes', *Curr. Sci.*, 2003, **85**, pp. 162–170
- Gopinatha, V., MubarakAlib, D., Priyadarshinia, S., *et al.*: 'Biosynthesis of silver nanoparticles from *Tribulus terrestris* and its antimicrobial activity: a novel biological approach', *Colloids Surf. B, Biointerfaces*, 2012, **96**, pp. 69–74
- Kumar, K., Srivastava, R., Neelam, R., *et al.*: 'Synthesis, characterization and antibacterial activity of silver nanoparticles against *S.aureus* (MTCC 87) and *P. aeruginosa* (MTCC 741) pathogens', *J. Pharmacy Res.*, 2012, **5**, pp. 841–844
- McCutcheon, A.R., Ellis, S.M., Hancock, R.E.W., *et al.*: 'Antifungal screening of medicinal plants of British Columbian native people', *J. Ethnopharmacol.*, 1994, **44**, pp. 157–169
- Sanjay, R., Ponmurugan, P., Baby, U.I.: 'Evaluation of fungicides and biocontrol agents against grey blight disease of tea in the field', *Crop Prot.*, 2008, **27**, pp. 689–694
- Balasuubramanian, S., Netto, L.A., Parathiraj, S.: 'Unique graft combination of tea, Cr-6017/UPASI-9', *Curr. Sci.*, 2010, **98**, pp. 1508–1517
- Han, G., Martin, T.C., Rotello, M.V.: 'Gold nanoparticle-bound DNA toward biological, physical, and chemical agents', *Chem. Biol. Drug Des.*, 2006, **67**, pp. 78–82

- [18] Dinesh, S., Karthikeyan, S., Arumugam, P.: 'Biosynthesis of silver nanoparticles from *Glycyrrhiza glabra* root extract', *Arch. Appl. Sci. Res.*, 2012, **4**, (1), pp. 178–187
- [19] Chitra, K., Annadurai, G.: 'Fluorescent silica nanoparticles in the detection and control of the growth of pathogen', *J. Nanotech.*, 2013, Article ID 509628, pp. 1–7, doi:10.1155/2013/509628
- [20] Badri Narayanan, K., Sakthivel, N.: 'Coriander leaf mediated biosynthesis of gold nanoparticles', *Mater. Lett.*, 2008, **62**, pp. 4588–4590
- [21] Khatami, M., Pourseyedi, S., Khatami, M., *et al.*: 'Synthesis of silver nanoparticles using seed exudates of *Sinapis arvensis* as a novel bioresource, and evaluation of their antifungal activity', *Bioresour. Bioprocess.*, 2015, **2**, (19), pp. 1–7
- [22] Soltani Nejad, M., Shahidi Bonjar, G.H., Khaleghi, N.: 'Biosynthesis of gold nanoparticles using *Streptomyces fulvissimus* isolate', *Nanomed. J.*, 2015, **2**, (2), pp. 153–159
- [23] Banala, R.R., Nagati, V.B., Karnati, P.R.: 'Green synthesis and characterization of *Carica papaya* leaf extract coated silver nanoparticles through X-ray diffraction, electron microscopy and evaluation of bactericidal properties', *Saudi J. Biol. Sci.*, 2015, **22**, pp. 637–644
- [24] El-Batal, A.I., Hashem, A.A.M., Abdelbaky, N.M.: 'Gamma radiation mediated green synthesis of gold nanoparticles using fermented soybean garlic aqueous extract and their antimicrobial activity', *Springer Plus.*, 2013, **2**, (129), pp. 1–10
- [25] Chang, K.F., Hwang, S.F., Wang, H., *et al.*: 'Etiology and biocontrol of Sclerotinia blight of coneflower using *Trichoderma* species', *Plant Pathol. J.*, 2006, **5**, pp. 15–19
- [26] Azam, A., Ahmed, F., Arshi, N., *et al.*: 'Stability of one step synthesis and characterization of gold nanoparticles and their antibacterial activities against *E. coli* (ATCC 25922 strain)', *Int. J. Theor. Appl. Sci.*, 2009, **1**, pp. 1–4
- [27] Fernando, W.G.D., Nakkeeran, S., Zhang, Y., *et al.*: 'Biological control of *Sclerotinia sclerotiorum* (Lib.) de Bary by *Pseudomonas* and *Bacillus* species on canola petals', *Crop Prot.*, 2007, **26**, pp. 100–107
- [28] Sapkal, M.R., Deshmukh, A.M.: 'Biosynthesis of gold nanoparticles by *Streptomyces* species', *Res. J. Biotech.*, 2008, **3**, pp. 36–39
- [29] Dadrick, C., da Silva, F.G., Shen, Y., *et al.*: 'Antagonistic interactions between strains of *Xanthomonas oryzae* pv. *oryzae*', *Phytopathology*, 2003, **93**, pp. 705–711
- [30] Morones, J.R., Elechiguerra, J.L., Camacho, A., *et al.*: 'The bactericidal effect of silver nanoparticles', *Nanotechnology*, 2005, **16**, pp. 2346–2353
- [31] Kim, H., Kang, H., Chu, G., *et al.*: 'Antifungal effectiveness of nanosilver colloid against rose powdery mildew in greenhouses', *Solid State Phenom.*, 2008, **135**, pp. 15–18